Supporting Information

Cu_2ZnSnS_4 Nanocrystal Dispersions in Polar Solvents

B. Selin Tosun, Boris D. Chernomordik, Aloysius A. Gunawan, Bryce Williams, K. Andre Mkhoyan, Lorraine F. Francis and Eray S. Aydil*

Department of Chemical Engineering and Materials Science, University of Minnesota, 421 Washington Avenue SE, Minneapolis, Minnesota 55455, USA

Experimental Procedures

Extraction **-** The CZTS nanocrystals were synthesized as described by Khare *et al.* (reference 14 in the manuscript) and dispersed in toluene. Typically, ~10 µl of oleic acid was added to the toluene dispersion to increase the shelf life of the dispersion in toluene. To extract these nanocrystals into formamide, 2 mL of formamide was mixed with either 100 µL of 1.28 g/mL or 150 µL of 1.92 g/mL K_2S solution in deionized water and added to 1 mL of CZTS nanocrystals (~ 2 mg/mL) dispersed in toluene. The two different amounts of K_2S correspond to 0.061 and 0.134 g/ml K_2S concentration in the polar solvent phase (> 93% by volume formamide and <7% by volume water). The two-phase mixture was stirred vigorously for 20, 60 or 180 minutes. In some experiments, we also carried out this step up to 16 hours. The transfer of nanocrystals to the formamide phase was detected visually. The solution with the CZTS nanocrystals appears black. While the formamide phase begins to get darker after stirring for 20 minutes, a thick emulsion remains visible between the polar and nonpolar phases, indicating incomplete extraction. Stirring longer slowly thins the emulsion and the formamide phase gets darker. After the stirring is stopped 1 mL toluene is added to the mixture and the polar and non-polar phases are allowed to separate by letting the vial sit for 5 minutes. Separation and breaking of the emulsion is easier for those extractions where the mixture has been stirred for one hour or longer. Emulsion completely disappears if the stirring is carried out for 16 hours. We believe that the nanocrystals covered with both alkly ligands and S^{2-} stabilizes the emulsion at the toluene-formamide interface. When the nanocrystals are mostly covered with S^{2-} they prefer to transfer to the formamide phase and the emulsion breaks up. Following, the toluene phase is removed from the top using a pipette and the nanocrystals are separated by precipitation from formamide containing K_2S by the addition of 2 mL of acetonitrile and centrifuging. The supernatant is decanted and the particles are redispersed in 2 ml of fresh formamide by vortexing and sonicating for a minute, each. This is the first step of the cleaning procedure. In a second cleaning step, the CZTS nanocrystals are again precipitated out of formamide by the addition of 2 mL each of acetonitrile, acetone and toluene. The liquid phase is decanted after centrifugation, and the nanocrystals are redispersed in 2 ml of formamide. This cleaning step can be repeated as

many as six times and removes excess K_2S. In the final step, the particles are dispersed either in formamide or DI water by sonication.

XRD and Raman Characterization - The nanocrystals are drop cast and dried on bare or molybdenum-coated Si (100) substrates for structural characterization with X-Ray Diffraction (XRD) and Raman spectroscopy. The drop-cast CZTS nanocrystal films from toluene were dried in air, at ambient conditions, while the nanocrystal films cast from formamide and DI water were dried in vacuum at ambient temperature. The nanocrystal films cast from formamide were dried for 10 hours, while those cast from DI water were dried for 1 hour. Even when the films after cast from dispersions that were prepared by cleaning the nanocrystals three times, there is still excess K_2S in the dispersions and one could observe K_2S crystals on the CZTS nanocrystal films. These crystals were removed by rinsing the film with ~10 mL of DI water and drying the film again in vacuum before all XRD and Raman measurements.

Raman Spectra were collected using a Witec Alpha300 R confocal Raman microscope. Raman scattering from an Argon ion laser (514.5 nm) was collected using a UHTS300 spectrometer that consisted of a monochromator with 1800 lines/mm grating and a DV401 CCD detector. Accumulation time was 1 second per frameand the scattered intensity was integrated for 10 frames with 0.02 cm^{-1} spectral resolution.

XRD patterns from drop cast films were collected and recorded using a Bruker-AXS microdiffractometer equipped with a Cu-K_α X-ray source using 0.8 mm spot size.

Transmission Electron Microscopy – CZTS suspensions (0.03 mg/ml) were dropcast on carbon grids for Transmission Electron Microscopy (TEM) characterization. The specimen grids were stored overnight under 10^{-8} Torr vacuum to remove the residual solvent prior to loading the grids into the microscope. Transmission electron microscopy (TEM) analysis was conducted using an FEI Tecnai F-30 microscope with a Schottky field-emission electron gun operated at 200 keV.

Attenuated Total Reflection Fourier Transform Infrared Spectroscopy (ATR-FTIR) - The ligand coverage on the surfaces of the CZTS nanocrystals was determined using ATR-FTIR spectroscopy. The spectra were collected using Nicolet Magna 550 Spectrometer equipped with an ATR-FTIR attachment (Harrick Scientific). Fixed and identical volumes (~300 μL) of colloidal CZTS suspensions in identical concentrations (~2 mg/mL) were cast onto a trapezoidal-shaped (45^o bevels) Ge ATR crystal (5 × 1 × 0.1 cm^3) and allowed to dry until all the solvent phase infrared absorptions disappeared and the nanocrystal films appeared dry. For NC films cast from dispersions in water and toluene, this typically took 1 hour. For NC films cast from dispersions in formamide, the Ge ATR crystal was dried in vacuum

overnight. Spectra were collected in the differential mode where the spectrum of the NC film is referenced with respect to the spectrum of the bare ATR crystal. In all cases enough nanoparticles were put on the ATR crystal such that the entire surface of the crystal (5 cm^2) was covered with a NC film and the film thickness was much larger than the penetration depth of the infrared radiation at 1000 cm^{-1} and above. That the film thickness had reached sufficient thickness was checked by doubling the NCs on the film and observing that the infrared spectrum and the intensities changed less than ~5%.

Absolute surface coverage of the ligands was estimated as follows. The absorbance of the ligand (oleic acid and oleylamine) was recorded by forming a liquid film on the Ge ATR crystal. When the film is thicker than the penetration depth the absorbance is given by

$$A_{\mathrm{l}} = N_{\mathrm{l}} \varepsilon A_{ATR} d_p^{\mathrm{l}} \tag{1}$$

where A_{l} is the absorbance of the liquid, N_{l} is the concentration of the liquid (*e.g.,* $N_{\mathrm{l}} = 1.83 \times 10^{21}$ molecules/cm^3 for oleylamine and $N_{\mathrm{l}} = 1.91 \times 10^{21}$ molecules/cm^3 for oleic acid), ε is the absorptivity, A_{ATR} is the surface area of the ATR crystal and d_p^{l} is the infrared penetration depth into the liquid. For a nanocrystal film cast on to the ATR crystal

$$A_{NC} = N_s \varepsilon A_p \tag{2}$$

where A_{NC} is the absorbance of the ligands on the nanocrystals surface, N_s is the surface coverage of ligands per unit area and A_p is the total surface area of the nanocrystals. Assuming spherical nanocrystals with radius r and a solid packing fraction, f_s, equation 2 can be written as

$$A_{NC} = \frac{3 N_s f_s \varepsilon A_{ATR} d_p^{NC}}{r} \tag{3}$$

where d_p^{NC} is the infrared penetration depth into the nanocrystal film. Both A_{NC} and A_{l} are experimentally measurable quantities at characteristic absorption frequencies of the ligand molecules. Taking the ratio of equations 1 and 3 and assuming that the absorptivity of the ligand in liquid and when it is adsorbed onto the nanocrystal surface are the same, one obtains an expression for the surface coverage of the ligand molecules as

$$N_s = \frac{N_{\mathrm{l}} A_{NC} r d_p^{\mathrm{l}}}{3 A_{\mathrm{l}} f_s d_p^{NC}}. \tag{4}$$

The penetration depth in film *i* depends on the absorption wavelength, λ and the refractive index of the film, n_i, and can be calculated from

$$d_p^i = \frac{\lambda}{2\pi\, n_{Ge}\sqrt{\sin^2\theta - (n_i/n_{Ge})^2}} \tag{5}$$

where θ is the total internal reflection angle. The refractive index of the nanocrystal film, n_{Ge}, is also a function of the packing fraction and can be calculated by assuming that it is a mixture of voids and CZTS using the Bruggeman effective medium theory. Thus, the only unknown in equation 4 is the solid packing fraction, f_s, which determines the quantity $d_p^{\mathrm{I}} / f_s d_p^{NC}$. This quantity is plotted as a function of the solid packing fraction, f_s in Figure SI-1 for Ge as the ATR crystal. If the nanocrystals pack randomly then solid packing fraction is 0.63 and the quantity $d_p^{\mathrm{I}} / f_s d_p^{NC}$ is 1.35. Thus, the surface coverage in ligand molecules per unit area can be calculated from

. This

$$N_s = 0.45\, N_{\mathrm{I}}\; r\, \frac{A_{NC}}{A_{\mathrm{I}}} \tag{6}.$$

A fractional coverage can be estimated by dividing this value by the site density of either the cations or the anions on (001) planes, 6.8×10^{14} cm^{-2}.

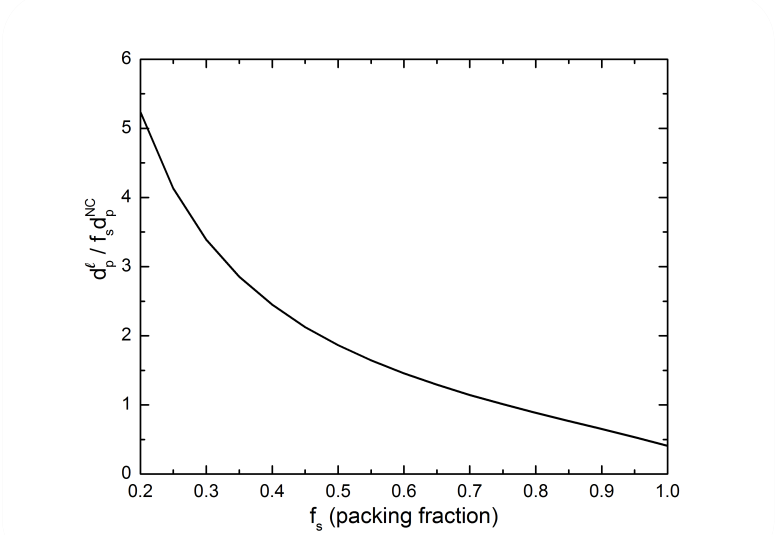

Figure SI-1: The quantity $d_p^{\mathrm{I}} / f_s d_p^{NC}$ in equation 4 as a function of the solid packing fraction, f_s.

Dynamic Light Scattering Measurements (DLS) – Nanocrystal size distributions were determined using dynamic light scattering (Brookhaven ZetaPLUS) after diluting the typical dispersions to 0.1 mg/ml. The light wavelength was 657 nm and scattering was collected perpendicular to the laser propagation direction. Ten independent 45-second long consecutive measurements were combined to obtain the final log-normal size distributions shown in Figure SI-2.

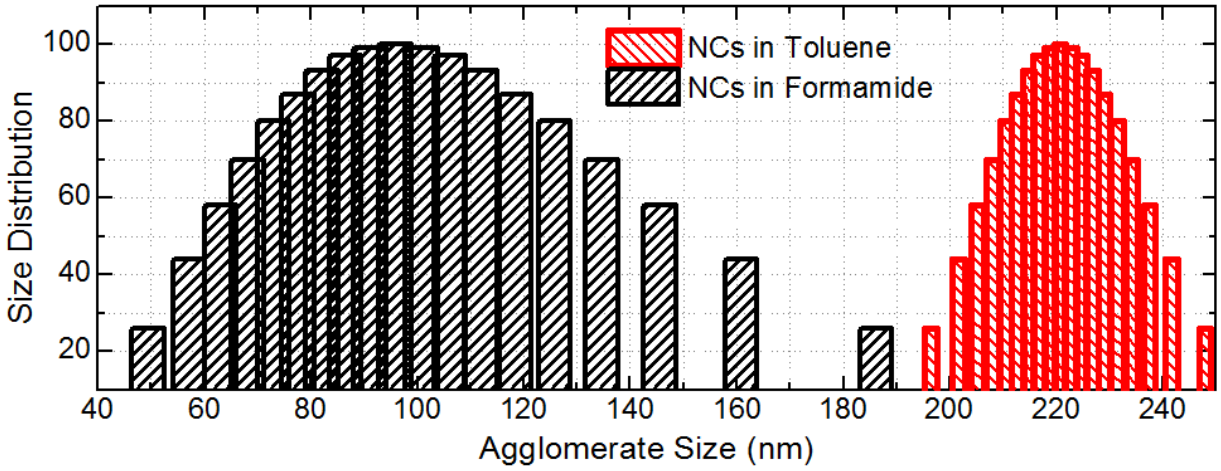

Figure SI-2: The size distributions of CZTS nanocrystals dispersed in toluene, before extraction and in formamide, after extraction.

Infrared Absorption Assignments – The major infrared absorptions in Figure 5 can be assigned to vibrations in K_2SO_4, $KHSO_4$ and in CH_2 and CH_3 groups in the oleic acid ligands that remain on the surface even after extraction into the polar solvent. Figure SI-3 shows the locations of these major absorptions and Table SI-1 lists their respective assignments based on literature. This data indicates that the surface of the air-dried CZTS nanocrystal is comprised of a combination of K_2SO_4, $KHSO_4$ in addition to the remaining oleic acid ligands.

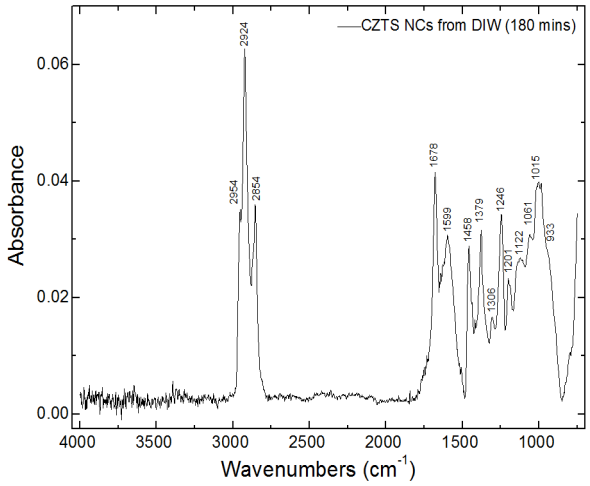

Figure SI-3: ATR-FTIR spectra of the CZTS nanocrystals drop cast from DI water with major infrared absorption peaks identified.

Table SI-1. Infrared absorption peak assignments for CZTS nanocrystals cast from water dispersions (See also Figure SI-3).

This Work (cm^{-1})	Literature value[reference]	Assignment
2954	2954[1-4]	C-H stretching in CH_3 in oleic acid and oleylamine
2924	2922[1-4]	C-H asymmetric stretch in CH_2 in oleic acid and oleylamine
2854	2854[1-4]	C-H symmetric stretch in CH_2 in oleylamine and oleic acid
1678	1647[3], 1650[4]	C=O stretching of oleic acid and possible contribution from C=C stretching
1599	1450-1700[2,3]	Asymmetric stretch of the COO^- metal bidentate on the CZTS surface, possible contribution from oleylamine NH_2 scissoring mode at 1590-1600
1458	1463[4]	CH_2 deformation (δ) modes in oleic acid ligands
1379	1379[5]	CH_3 umbrella mode in oleic acid
1306	1292-1326[6]	SO asymmetric stretching in $KHSO_4$
1246	1255[6,7]	S-OH plane bending in $KHSO_4$
1201	1200[6,7]	Asymmetric SO_3 vibrations in HSO_4^-
1122	1080-1125[6-10]	Asymmetric SO_4 stretching in K_2SO_4 and $KHSO_4$
1061	1060[9,10]	Symmetric stretching of SO_4 group in $KHSO_4$
1015	1015[9,10]	Symmetric stretching of SO_4 group in $KHSO_4$
930	932[8,9]	Symmetric stretching of SO_4 group in $KHSO_4$ and K_2SO_4

1. J. M. Luther, M. Law. Q. Song. C. L. Perkins, M. C. Beard and A. J. Nozik, *ACS Nano*, 2008, **2**, 271.
2. N. Wu, L. Fu, M. Su, M. Aslam, K. C. Wong and V. P. Dravid, *Nano Lett.*, 2004, **4**, 383.
3. N. Shukla, C. Liu, P. M. Jones and D. Weller, *J. Magn. Magn. Mater.*, 2003, **266**, 178.
4. P. J. Thistlewaite and M. S. Hook, *Langmuir*, 2000, **16**, 4993.
5. R. Efrat, Z. Abramov, A. Aserin, and N. Garti, *J. Phys. Chem. B*, 2010, **114**, 10709.
6. A. Gopiyron, J. Devillepin and A. Novak, J. Raman Spectrosc., 1980, **9**, 297.
7. T. Senna, N. Ikemiya and M. Ito, *J. Electroanalytical Chem.* 2011, **511**, 115.
8. F. El-Kabbany, G. Said, Y. Badr, S. Taha, Phys. Sat. Sol. (a), 1981, **67**, 339.
9. J. Baran, *J. Mol. Struct.,* 1988, **172**, 1.
10. Y. Sawatari, T. Sueoka, Y. Shingaya and M. Ito, *Spectrochimica Acta*, 1994, **50A**, 1555.